7th International Symposium on Cavitation
CAV2009
August 17-22, 2009, Ann Arbor, Michigen, UAS

OBSERVATIONS AND NUMERICAL SIMULATIONS OF UNSTEADY PARTIAL CAVITATION ON 2-D HYDROFOIL

Xiaoxing Peng, Guoping Zhang, Bin Ji*, Linzhang Lu, Fangwen Hong
China Ship Scientific Research Center
P.O.Box 116, Wuxi, Jiangsu, 214082, P. R. China
me04px@alumni.ust.hk

ABSTRACT

In present paper, experimental observations and numerical simulations are used to understand some flow mechanism of partial cavity, such as the instability of attached sheet cavitation and the relations between cloud cavitation and erosion. NACA0012 and NACA16012 hydrofoils were employed both as the test model in the cavitation tunnel experiments and the model for numerical simulations. The high-speed video camera and TR-PIV system was used in the experiments. The re-entrant jet was captured successively in experiment and the mechanism that the re-entrant jet induced the break-off of cavity is validated. In numerical simulation, Reynolds-Averaged Navier-Stokes equations with the cavitation model of Transport Equation Model (TEM) were developed. The cavity morphology, flow structure, instability and developing process, were investigated. The numerical results showed that re-entrant jet is not absolutely constituted by liquid but vapor/liquid mixture, and the break-off process of sheet cavitation is directly induced by re-entrant jet closely along the wall. The calculating shedding frequencies are very close to the experimental data.

INTRODUCTION

The partial cavitation often occurs in various application areas, such as hydrofoils, propellers and pumps. The researches of unsteady partial cavitation have being received great attentions due to its strong relations with vibration, noise and cavitation erosion. To avoid and control the severe damage of partial unsteady cavitation to hydraulic systems many research works have been done to study the complex features of unsteady partial cavitation, specially the cause of instability. Previous studies indicated that re-entrant jet at the end of the cavity seems commonly to be considered as the one of the main mechanism of cavity destabilization and cloud cavitation formation. Several other mechanisms were also proposed such as shock wave of bubbly flow, surface instability of sheet cavity, transitional instability from partial cavitation to super cavitation, and so on. However, up to now the basic physics of cavity destabilization and transition to cloud cavitation is still progressing and need to be documented.

In fact the understanding of unsteady nature of partial cavitation strongly depend on the experimental observation, which may bring out the find of new mechanism and the validation of new theory. The recent development of experimental methods such as high-frame rates video measurement and time-resolved PIV (TR-PIV) allows us to observe and measure more details of unsteady partial cavitation. In other hand, with the increase of computational power methods more general and flexible multiphase flow models were proposed in the last decade. The combinations of multiphase flow models with RANS simulations offer us a better perspective of modeling more details of cavitation and its consequences.

In this paper, some recent results of experimental observations and numerical simulations are presented. The purpose of the investigation was to observe and research in some detail the cavitation behavior of partial cavitation. Several two dimensional hydrofoil were employed as the test model in the cavitation tunnel experiments and also as the model for numerical simulations.

EXPERIMENT AND OBSERVATION

The experiments were carried out in the caviation tunnel in China Ship Scientific Research Center (CSSRC). Two 2-D hydrofoils, NACA0012 and NACA16012 were used as test models. The materials of the two hydrofoils were aluminum alloy with parint on the surface. The model of NACA0012 with the chord length 200mm and the span 500mm was test in ϕ 800mm cavitation tunnel, while model of NACA16012 with the chord length100mm and the span 342mm was test in ϕ350mm cavitation tunnel. The high-speed video camera with frame rate up to 5000 frames/second was used to investigate the unsteady process of cavitation flow around. A CCD camera with resolution 2k×2k were used to capture the detail of the cavity. A TR-PIV system with space

* Bin Ji now is a PhD student of Tsinghua University

resolution 1k×1kpixel@2kHz was also used in the experiments to study the variation of the cavity and flow around it.

The re-entrant jet was captured successively in experiment and the mechanism that the re-entrant jet induced the break-off of cavity is validated. Figure 1 shows some results obtained by the high speed camera. The test model is NACA0012 hydrofoil with attack angle $\alpha = 8^0$, incoming velocity v=8m/s, cavitation number δ=1.2. The time interval of each frame is 2ms. The observation also indicated the shedding cloud cavitation often could stay for a time on the hydrofoil and the erosion may occur in that area.

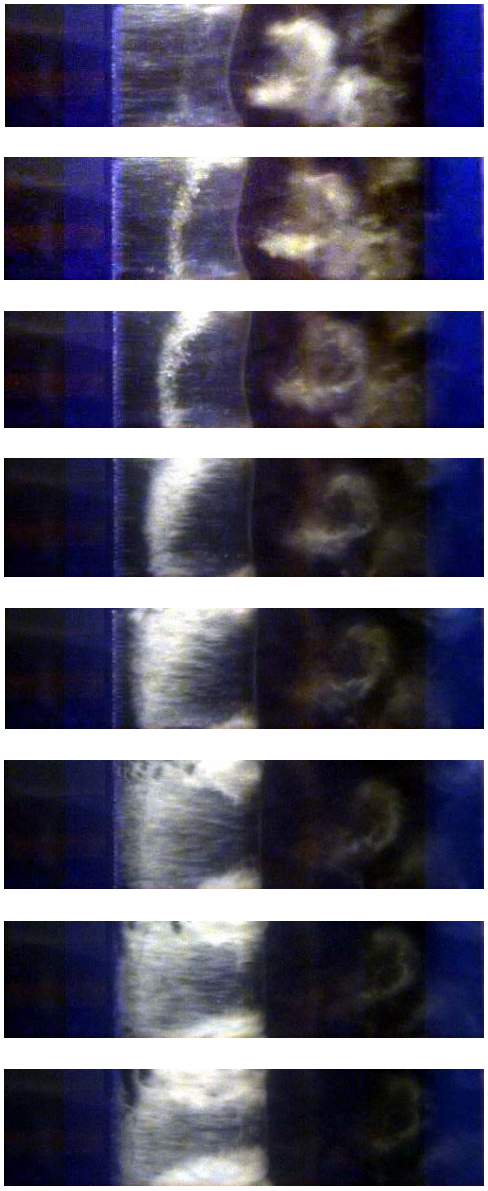

Fig. 1 Process of re-entrant jet in NACA0012 with 2ms interval between each frame, flow from left

($\alpha = 8^0, V = 8m/s, \delta = 1.2$)

The observation from high speed camera also illustrates that the shedding of cloud caviation in this case has a periodic behavior. The shedding frequency can be presented by Strouhal number $St = \frac{f \times L_{\max}}{V\sqrt{1+\sigma}}$, where f is the frequency of shedding, $L_{\max}$ is the maximum length of sheet cavity, V is the velocity of incoming flow. In this case the St=0.19.

It should be pointed out pictures shown in Figure 1 are only part of hydrofoil span, to focus the re-entrant jet process. In fact the cavity in the 2-D hydrofoil almost is three dimensional. Figure 2 shows an example obtained from CCD camera. It clearly indicates that direction of re-entrant jet is vertical to trailing edge of sheet cavity. Also the development of sheet cavity and the shedding of cloud cavitation are quite complicated along the span of the foil. In same case the re-entrant flow generates shedding while at the same time its front continues upstream.

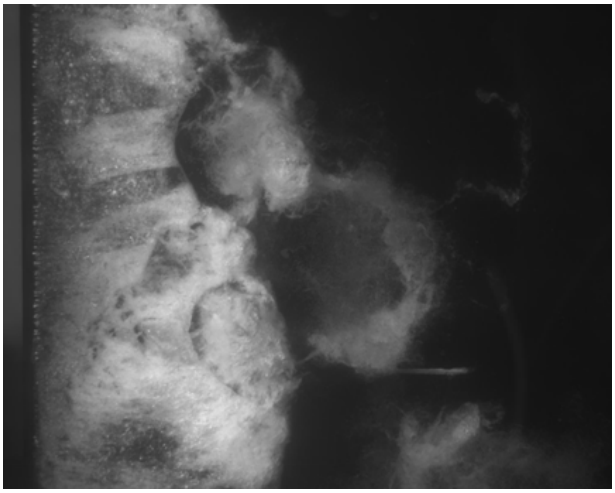

Fig. 2 Three dimensional shedding and the direction of re-entrant jet, NACA0012, flow from left

($\alpha = 8^0, V = 8m/s, \delta = 1.2$)

Observations from the side of the profile show that the shed cloud becomes very thick as shown in Figure 3 both (a) and (b) . The question is which mechanism moves the gas or cavity structure so far away from the foil surface. This movement away from the foil may also occur quite far upstream, as shown in Figure 3 (b). The explanation may be derived from the mechanism of re-entrant flow. A strong re-entrant flow, especially when is converging, will not only become thicker, but the collision between converging flow directions will also created an outward directed flow component. When the impulse of this component is high, the re-entrant flow will shoot through the surface of the cavity. This creates a jet perpendicular to the foil

surface into the fluid. Since the jet comes from a vapor environment clouds of vapor will be entrained. Such a mechanism can generate a cloud of vaporous bubbles in the fluid, which is many times thicker than the sheet cavity.

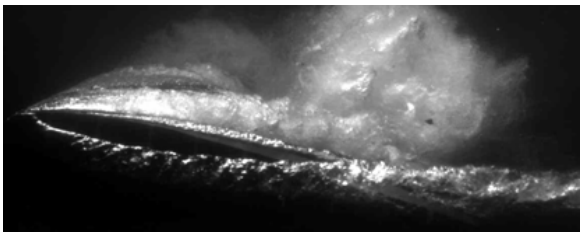

(a)

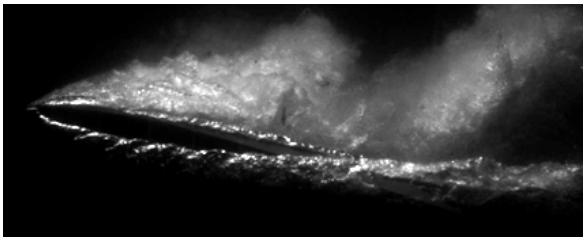

(b)

.

Fig. 3 Side views of cavitation in NACA0012, flow from left

($\alpha = 8^0, V = 8m/s, \delta = 1.0$)

Some exploring experiments of TR-PIV system were made to try to get some time series of cavitation devolvement and the flow field around the cavity. The contours of cavity and PIV particle image were obtained after several post-processes, such as minimum filtration, Guess faintness, as well as separation and combination of the image. Figure 4 shows an example of the time evolution of cavity shape, where the test model is NACA16012 hydrofoil with attack angle $\alpha = 8^0$, incoming velocity v=7m/s, cavitation number δ =0.94. The time interval of each frame is 2ms. The maximum length of attached cavity can be estimated to 70mm. The shedding frequency presented by Strouhal number is about St =0.24

From the post-process of PIV measurement the flow field including velocity distribution and vorticity distribution near the cavity also can be obtained as shown in Figure 5. It mast pointed out the present results are still preliminary and qualitative due to it is difficult to treat the relation between PIV particles and the cavity in illumination, especially near the boundary of cavity. But the results also show us that the velocity direction near the cavity is almost along the boundary and the strong vortex exists around the shedding cavity.

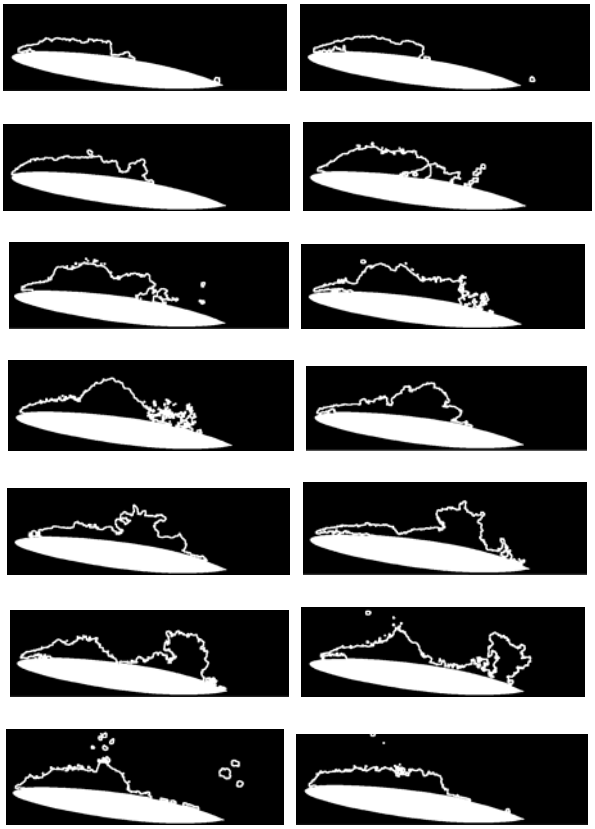

Fig. 4 The development of cavity contours obtained by TR-PIV, NACA16012, flow from left

($\alpha = 8^0, V = 7m/s, \delta = 0.94$)

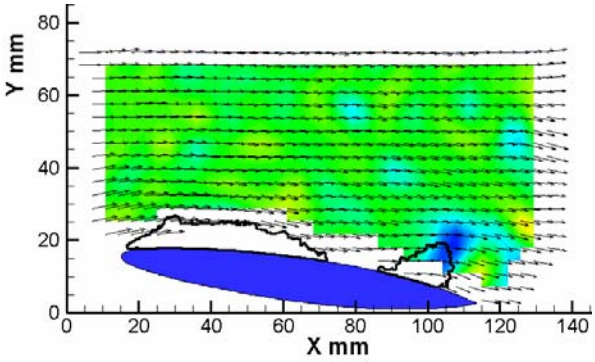

Fig. 5 The velocity and vorticity distribution near the cavity obtained from PIV, NACA16012, flow from left

($\alpha = 8^0, V = 7m/s, \delta = 0.94$)

NUMERICAL SIMULATION

Physical model of Cavitation

The present work applies a single-fluid model. Two cavitation model, the state equation model and transport equation mode (TEM) are tried in our numerical simulation. But the following results is

obtained by TEM.

The phase transport equation is applied to model the phase change between liquid and vapor in TEM and its density transport equation can be shown as

$$\frac{\partial}{\partial t}(\rho f_v)+\frac{\partial}{\partial x_j}(\rho u_j f_v)=m^+-m^- \qquad (1)$$

where, ρ is the density of mixture, f_v is the density fraction of vapor, m^+、m^- are the density source of evaporation and condensation in per mixture volume respectively.

It is great effect on the simulation results of how to determine the density source. In present work the following equations are introduced.

$$m^+=C_e\frac{\rho_l}{\rho_v}\frac{Max(p_v-p,0)}{0.5\rho_l V_\infty^2 t_\infty\sqrt{T}}(1-f_v) \qquad (2)$$

$$m^-=C_c\frac{\rho_l}{\rho_v}\frac{Max(p-p_v,0)}{0.5\rho_l V_\infty^2 t_\infty\sqrt{T}}f_v \qquad (3)$$

where, t_∞ is non-dimensional time, V_∞ is the incoming velocity, p is the local pressure, T is the temperature, ρ_v is vapor pressure, C_e and C_c are coefficients of evaporation and condensation respectively. In this paper C_e =50 and C_c =5000 from the former experimental calibration

Control equation

The simulations are based on 2-D calculations of the flow. The mass and momentum equations are solved.

$$\frac{\partial\rho}{\partial t}+\frac{\partial(\rho u_j)}{\partial x_j}=0 \qquad (4)$$

$$\frac{\partial(\rho u_i)}{\partial t}+\frac{\partial(\rho u_i u_j)}{\partial x_j}= -\frac{\partial p}{\partial x_i}+\frac{\partial}{\partial x_j}[(\mu+\mu_t)(\frac{\partial u_i}{\partial x_j}+\frac{\partial u_j}{\partial x_i}-\frac{2}{3}\frac{\partial u_k}{\partial x_k}\delta_{ij})] \qquad (5)$$

where μ is dynamic viscosity and μ_t is turbulent viscosity. The mixture density ρ and dynamic viscosity μ can be determined by

$$\rho=\rho_v\alpha_v+\rho_l(1-\alpha_v) \qquad (6)$$

$$\mu=\mu_v\alpha_v+\mu_l(1-\alpha_v) \qquad (7)$$

where α_v represents the volume fraction of vapor and shown as:

$$\alpha_v=\frac{\rho f_v}{\rho_v} \qquad (8)$$

Turbulence model

A appropriate turbulence model is very important for the simulations of unsteady cavitation, especially for cloud cavitation. In present paper k-ε RNG model was used.

$$\mu_t=f(\rho)\rho_l C_\mu\frac{k^2}{\varepsilon} \qquad (9)$$

The function $f(\rho)$ is expressed as following:

$$f(\rho)=\left[\rho_v+\left(\frac{\rho_v-\rho}{\rho_v-\rho_l}\right)^n(\rho_l-\rho_v)\right]/\rho_l \qquad (10)$$

with $n=10$.

Calculation results

NACA0012 and NACA16012 hydrofoils were used to study the unsteady features of partial cavitation in present numerical simulations. The flow conditions were selected so that the unsteady cavitation including partial cavity oscillations and large vapor cloud shedding can be obtained.

In the case of NACA0012 hydrofoil same chord length 200mm and same flow conditions, $\alpha=8^0$, v=8m/s, δ =1.2 with experiment are used in the numerical simulation. Figure 6 shows some typical states of one oscillation cycle. The maximum length of attached cavity can be estimated to about 100mm. The shedding frequency presented by Strouhal number is about St =0.19. These reproduce the experiment results quite well. The analysis of velocity field also found the re-entrain jet as shown in Figure 7. The re-entrain jet started as the cavity length reaches the maximum and upstream to the leading edge of the foil. It results in the break-off of attached cavity and formation of cloud caviation.

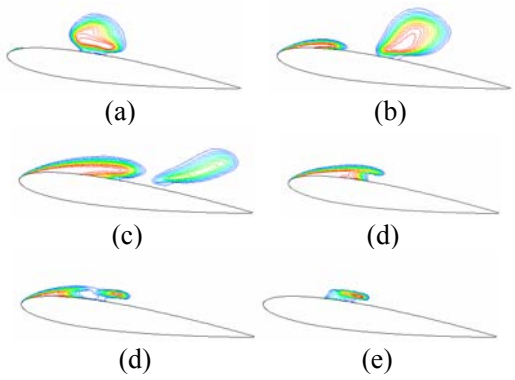

Fig. 6 Some typical states of of unsteady partial cavitation obtained by CFD, NACA0012, flow from left

($\alpha=8^0, V=8m/s, \delta=1.2$)

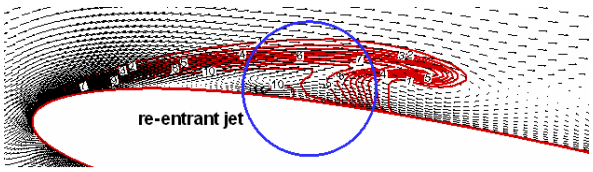

Velocity distributions in the state (d) of Fig.6

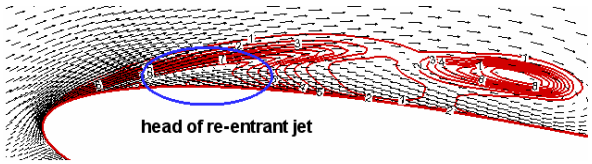

Velocity distributions in the state (e) of Fig.6

Fig. 7 Velocity distributions and re-entrain jets obtained by CFD, NACA0012, flow from left

$(\alpha = 8^0, V = 8m/s, \delta = 1.2)$

Figure 8 shows the complete cycle to display the successive steps of unsteady process, where hydrofoil is NACA16012 with chord 100mm and flow conditions are attack angle $\alpha = 8^0$, incoming velocity v=8m/s, cavitation number δ =0.9 similar to the experiment mentioned above. The maximum length of attached cavity can be estimated to 85mm. The shedding frequency presented by Strouhal number is about St =0.25, which is qualitative agreement with above experimental result.

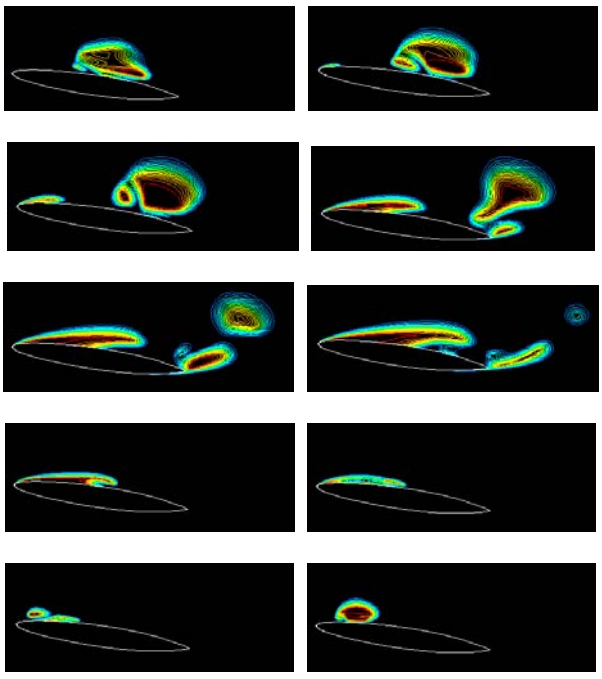

Figure 8 The successive steps of unsteady partial cavitation obtained by CFD, NACA16012, flow from left

$(\alpha = 8^0, V = 8m/s, \delta = 0.9)$

The flow field including velocity distribution and vorticity distribution around the hydrofoil also obtained. Figure 9 shows the velocity distribution (a) and vorticity distribution (b) in one of the steps of the unsteady partial cavitation process. In Figure 7 (a) the mixture density also presented. From these results the relation between cloud cavity shedding and vortex are clearly indicated.

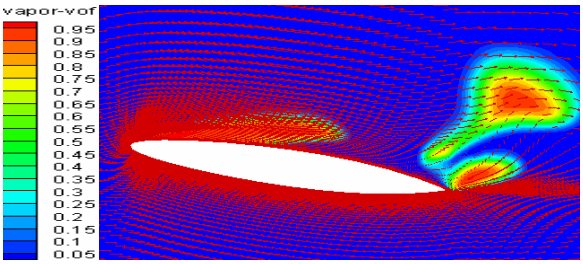

(a) Velocity distribution

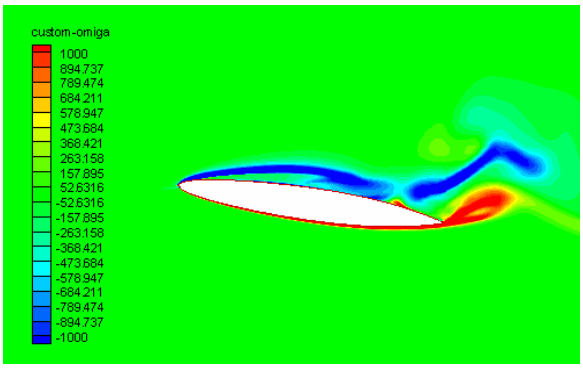

(b) Vorticity distribution

Fig. 9 Velocity and vorticity distribution around NACA16012

$(\alpha = 8^0, V = 8m/s, \delta = 0.9)$

CONCLUSION REMARKS

Some results of unsteady partial cavitation on two 2-D hydrofoils obtained by experiment observations and numerical simulations were presented in this paper.

In the experiment observation re-entrain jets were successfully captured. Through the shedding of could cavitation is a strongly three-dimensional phenomenon, but the mechanism of these shedding mainly initiated by converging re-entrant flow are validated.

From the side observation the shedding moves the cloud cavity further away from the foil surface than it seems possible by entrainment of the flow. This means that strong velocities perpendicular to the foil surface are generated and this can only be due to the converging re-entrant flow.

TR-PIV technique was used in the present research. The preliminary results show that the velocity direction near the cavity is almost along the boundary of

attached cavity and the strong vortex exists around the shedding cavity.

In numerical simulation, the present code was proved it can be simulate the total preference of unsteady partial cavitation such as the mechanism of re-entrain jet and the shedding frequency. The numerical results indicate that re-entrant jet is not absolutely constituted by liquid but vapor/liquid mixture, and the break-off process of sheet cavitation is directly induced by re-entrant jet closely along the wall. The calculating shedding frequencies are very close to the experimental data.

ACKNOWLEDGMENT

The authors wish to express their deep appreciation to Dr Gerrit Kuiper from MARIN for his help in the experiment analysis. The cavitation model used in the present paper was developed by Hydraulic Machinery Laboratory of Tsinghua University in Beijing.

REFERENCES

Coutier-Delgosha O., Deniset F., Leroux J., 'Numerical prediction of cavitating flow on a two-dimensional symmetrical hydrofoil and comparison to experiments', J. Fluids Eng., v129, pp.279-292, 2007

Coutier-Delgosha, Q., Fortes-Patella, R. and Reboud, J.L., 'Evaluation of the Turbulence Model Influence on the Numerical Simulation of Unsteady Cavitation', J. Fluid Eng., V125, pp. 38-45, 2003

Foeth, J-P, 'The structure of three-dimensional sheet cavitation', PhD thsis, MARIN, 2008

Franc, J-P,& Michel, J-M, 'Fundamentals of cavitation', Kluwer Academic Publishers, 2004

Franc, J-P, 'Partial cavity instabilities and re-entrain jet' CAV2001, Fourth International Symposium on cavitation, june 20-23, Pasadena, CA, UAS, 2001

Ji, B. Hong, F-W, Peng, X-X, 'The numerical analysis of shedding characteristics on partial cavitation over 2D hydrofoil", J. hydrodynamics, Ser. A, v23, No.4, 2008

Kawanami, Y., Kato, H., Yamaguchi, H., Tanimura, M. and Tagaya, Y., 'Mechanism and Control of Cloud Cavitation', J. Fluids Eng., v119, pp. 778-794, 1997

Kubota, A., Kato H. & Yamaguchi H., 'A new modeling of cavitating Flows: a numerical study of unsteady Cavitation on a Hydrofoil Section', J. Fluid Mech., v240, pp. 59-96, 1992

Leroux, J-B, Astolfi, J-A., Billard, Y., 'An experimental study of unsteady parital cavitation', ASME J. Fluid Eng., V126, pp. 94-101, 2004

Laberteaux, K-R, Ceccio, S-L, "partial cavity flow. Part1 cavities forming on models without spanwisw variation" J. Fluid Mech., V431, pp. 1-41, 2001

Pham, T.M., Larrarte, F. and Fruman, D.H., 'Investigation of Unsteady Sheet Cavitation and Cloud Cavitation Mechanisms', J. Fluid Eng., v121, pp. 289-296, 1999

Yamaguchi, H., 'Cloud Cavitation on Foil Sections', CAV2006, 6th International Symposium on Cavitation, Wageningen，The Netherlands, 2006